Cooling of a Multichip Electronic Module by Means of Confined Two-Dimensional Jets of Dielectric Liquid

D. C. Wadsworth
Graduate Research Assistant.

I. Mudawar
Associate Professor and Director.

Boiling and Two-Phase Flow Laboratory,
School of Mechanical Engineering,
Purdue University,
West Lafayette, IN 47907

Experiments were performed to investigate single-phase heat transfer from a smooth 12.7×12.7 mm² simulated chip to a two-dimensional jet of dielectric Fluorinert FC-72 liquid issuing from a thin rectangular slot into a channel confined between the chip surface and nozzle plate. The effects of jet width, confinement channel height, and impingement velocity have been examined. Channel height had a negligible effect on the heat transfer performance of the jet for the conditions of the present study. A correlation for the convective heat transfer coefficient is presented as a function of jet width, heater length, flow velocity, and fluid properties. A self-contained multichip cooling module consisting of a 3×3 array of heat sources confirmed the uniformity and predictability of cooling for each of the nine chips, and proved the cooling module is well suited for packaging large arrays of high-power density chips.

1 Introduction

The current trend of miniaturization of electronic components has given rise to alarmingly high power densities. Future technologies may result in power densities in excess of 100 W/cm² at the chip level by the mid-1990s (Bar-Cohen et al., 1986). This trend is complicated by a need for reduction in the dimensions of cooling hardware to facilitate three-dimensional packaging of multichip modules in a minimum volume.

Conventional methods of cooling, such as free and forced air convection, are no longer adequate for the anticipated fluxes. An alternative form of cooling, which has captured much attention in recent years, consists of direct immersion in dielectric liquids. This form of cooling circumvents the problem of high thermal resistance associated with previous technologies and offers the potential for greatly increasing the chip cooling rate. However, poor thermal transport porperties of dielectric liquids make it necessary to augment heat transfer by means of forced convection, surface enhancement, and/or phase change to meet projected chip cooling demands. Recent studies have shown that single-phase forced-convection cooling of chips in a channel is capable of meeting high-power chip cooling requirements (Samant and Simon, 1986; Ramadhyani and Incropera, 1987; Maddox and Mudawar, 1989; Mudawar and Maddox, 1989a, 1989b). Mudawar and Maddox (1989b) dissipated more than 200 W/cm² and 300 W/cm² using single and two-phase cooling, respectively, from an enhanced surface over which FC-72 (product of 3M) was forced at a moderate velocity while maintaining the chip temperature below 86°C.

Jet impingement, introduction of the cooling fluid perpendicular to the heated surface, has been employed in a variety of environments requiring continuous dissipation of enormous heat fluxes such as cooling of turbine blades, X-ray medical equipment, laser weapons, and annealing of steel. The attractive heat transfer characteristics of an impinging jet make this cooling configuration a viable candidate for the removal of very high power densities encountered in microelectronic devices.

Several jet impingement studies have been conducted using a circular orifice from which the coolant issued (Ma and Bergles, 1983; Jiji and Dagan, 1987). One drawback to such a configuration is the concentration of cooling in the small impingement zone of the heated surface. The use of multiple jets enhances cooling uniformity by creating several impingement zones that cover a significant fraction of the heated area. However, multiple jets promote flow blockage between the jets and complicate fluid distribution downstream from the impingement zone. As indicated in a literature survey by Downs and James (1987), the interference between circular jets leads to a reduction in heat transfer caused by the forma-

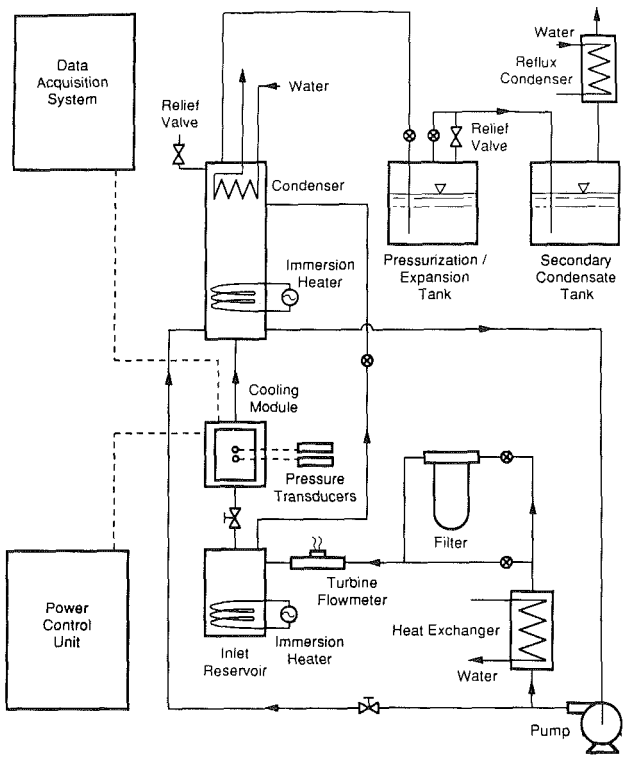

Fig. 1 Schematic diagram of the experimental facility

Contributed by the Heat Transfer Division for publication in the JOURNAL OF HEAT TRANSFER. Manuscript received by the Heat Transfer Division April 12, 1989; revision received February 9, 1990. Keywords: Electronic Equipment, Jets.

Copyright © 1990 by ASME
Downloaded 17 Jul 2012 to 128.211.160.35. Redistribution subject to ASME license or copyright; see http://www.asme.org/terms/Terms_Use.cfm

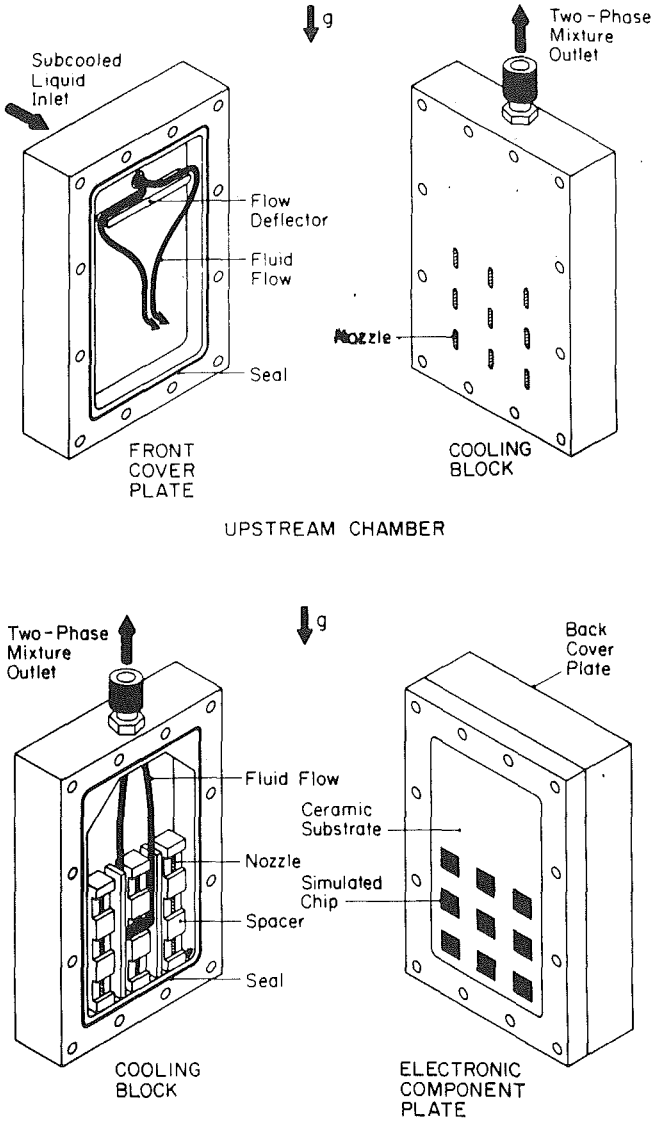

Fig. 2 Schematic diagram of the cooling module

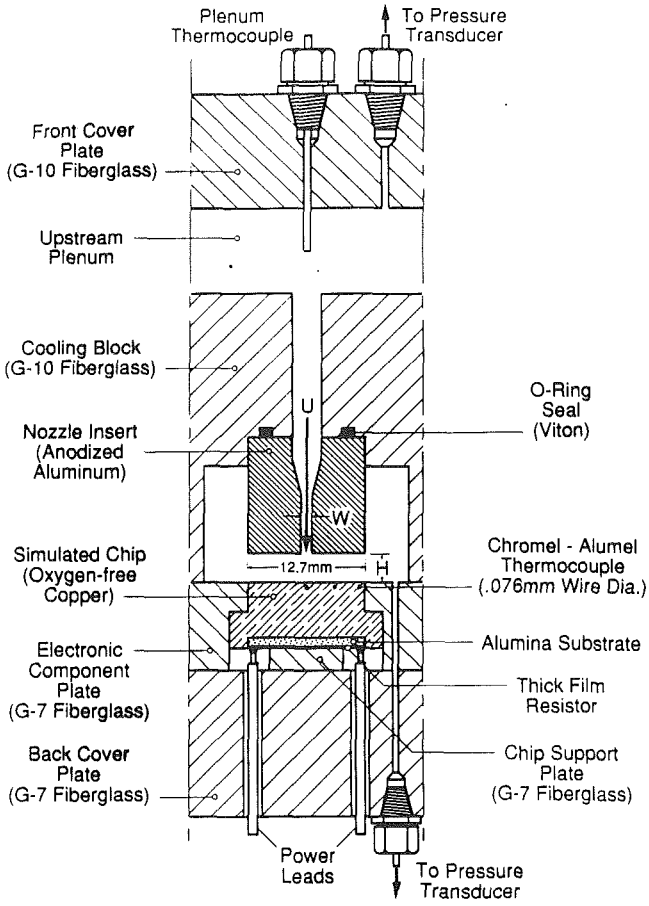

Fig. 3 Sectional view of the cooling module

tion of eddies, and to boundary layer separation, between adjacent jets. The complex spatial variations in the heat transfer coefficient associated with jet interference was illustrated by Goldstein and Timmers (1982) using flow visualization techniques. These problems become very critical in the cooling of multichip modules, which require uniform cooling of a large number of chips and ease of fluid introduction into, the rejection from, the module in the smallest volume possible. A potential solution to this problem is to use two-dimensional or slot jets, which provide a larger impingement zone and insure uniform coolant rejection following impingement.

This paper presents a packaging concept for cooling an array of heat sources (simulated chips) by means of a confined two-dimensional slot jet. Data are correlated for single-phase heat transfer from a smooth 12.7 mm × 12.7 mm chip to a jet of dielectric Fluorinert FC-72 liquid issuing from a thin rectangular slot into a channel confined between the chip surface and the nozzle plate. Information concerning the chemical and thermal properties of FC-72 can be found in previous papers by Mudawar and Maddox (1989a) and Mudawar and Anderson (1989).

Nomenclature

H = height of confinement channel

$\bar{h}_L$ = average heat transfer coefficient based on heater length $= q/(T_s - T_f)$

k = thermal conductivity of liquid based on mean liquid temperature

L = length of heater = 12.7 mm

$\overline{\mathrm{Nu}}_L$ = average Nusselt number based on heater length $= qL/(T_s - T_f)k$

Pr = Prandtl number of liquid based on mean liquid temperature

q = mean surface heat flux

Re = Reynolds number based on nozzle hydraulic diameter $= U(2W)/\nu$

Sc = Schmidt number

$\overline{\mathrm{Sh}}_L$ = mean Sherwood number based on heater length

T_f = liquid temperature at nozzle inlet

T_m = mean liquid temperature $= (T_s + T_f)/2$

T_s = mean temperature of heater surface

$\Delta T = T_s - T_f$

U = mean jet velocity at nozzle exit

W = nozzle width

x = horizontal distance along heater surface measured from centerline of impingement zone

ν = kinematic viscosity of liquid based on mean liquid temperature

Downloaded 17 Jul 2012 to 128.211.160.35. Redistribution subject to ASME license or copyright; see http://www.asme.org/terms/Terms_Use.cfm

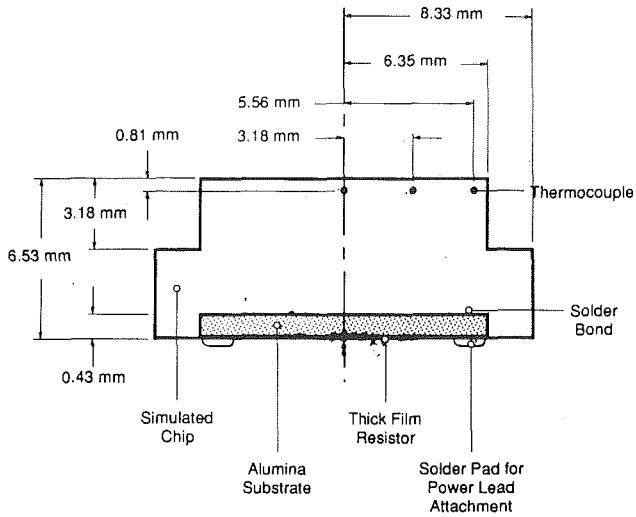

Fig. 4 Test heater construction

2 Experimental Apparatus and Procedure

A schematic diagram of the experimental facility used in this study is shown in Fig. 1. The flow loop was designed to accommodate both single-phase and two-phase experiments. The cooling module was installed between two fluid reservoirs equipped with internal immersion heaters.

Fluid in the system (FC-72) was circulated by a magnetically coupled centrifugal pump. A bypass line from the pump, connected in parallel with the cooling module, made it possible to regulate the flow through the cooling module even for very small flow rates. Flow rate through the test module was measured by a turbine flow meter. Accurate control of fluid temperature was achieved by two immersion heaters coiled in the upstream and downstream reservoirs of the cooling module, and a flat plate water-cooled heat exchanger located downstream from the pump. Two external tanks, shown in Fig. 1, were used for deaeration and for controlling pressure in the system.

Cooling Module. The cooling module accommodated a 3×3 array of 12.7 mm $\times$ 12.7 mm simulated chips. Coolant was supplied to each of the nine chips via a single isolated rectangular slot. As shown in Fig. 2, the module consisted of four parallel attachments: front cover plate, cooling block, electronic component plate, and back cover plate. Fluid was introduced into the module through the front cover plate. A flow deflector downstream from the inlet redistributed the flow and helped create uniform pressure in the chamber formed between the front cover plate and cooling block. The flow was distributed between the nine nozzles, from which fluid impinged onto the simulated chips flush-mounted in the electronic component plate. Fluid impingement was confined to a channel formed between the nozzle face and the simulated chip. After exiting the channel, the fluid was routed vertically upward to the cooling module outlet. The module was designed to insure cooling uniformity among the chips by producing a total pressure drop across the nozzle and confinement channel significantly larger than the pressure drop in the upstream chamber or outlet regions.

Figure 3 shows a detailed sectional view of the cooling module. Located in the front cover plate and extending into the upstream chamber was a single type K thermocouple for measurement of liquid inlet temperature. Also located in the front cover plate was a pressure port to which an absolute pressure transducer was attached. A second pressure port was placed at the confinement channel outlet. Pressure drop through the nozzle and confinement channel was measured by a differential pressure transducer connected between the two pressure ports.

The geometric characteristics of the impinging flow were changed by using different nozzle inserts, which were recessed into the G-10 cooling block. The anodized aluminum nozzle inserts consisted of a 30-deg converging entrance region followed by a straightening section five times the jet width. During single-chip tests, the liquid was injected only through the central nozzle while the other eight nozzles were blocked.

Heater Design. Figure 4 details the construction of the simulated chip. Three type K (chromel-alumel) thermocouples were used to instrument the test heater. Each thermocouple was constructed from 0.13-mm (5-mil) wire and insulated with a two-hole ceramic tube. The thermocouple assemblies were inserted into 0.79-mm (1/32-in.) diameter holes in the copper block to a depth of 6.35 mm. Machining and thermocouple location tolerances were maintained within ± 0.03 mm (1 mil). The thermocouple beads were coated with boron nitride thermally conducting epoxy. The thermocouples were located in a plane parallel to the chip surface and perpendicular to the plane of Fig. 4. One of the thermocouples was placed along the centerline of the chip corresponding to the impingement zone while the other two were distributed along the confinement channel flow direction as shown in Fig. 4. The heating element of the simulated chip was a commercially available 90-ohm thick film resistor. The resistor was supplied with a solder coating on the alumina backside for convenient bonding to the copper block. Power to the test heaters was supplied by a 240-vac variac. Power input was measured by means of voltage and current transducers.

Data were taken and recorded using a Keithley series 500 data acquisition system coupled to a Compaq 286 microcomputer. The data acquisition system monitored and processed signals from the current and voltage transducers, pressure transducers, and thermocouples. Thermocouple measurement resolution using this system was approximately 0.1°C.

Experimental Procedure. Deaeration of coolant in the system was necessary to insure consistency of fluid properties for the entire data base. At the onset of each test the coolant was deaerated by energizing the immersion heaters while circulating the fluid through the system. During dearation the fluid temperature was raised to approximately 60°C and maintained at that level for 20 minutes. During this time, air and coolant vapor were released from the upper reservoir into the pressurization tank and secondary condensate tank. A water-cooled reflux condenser connected to the secondary condensate tank permitted air to escape freely into the ambient as coolant vapor was being captured in the condensate tank. Following deaeration the valve connecting the pressurization tank and secondary condensate tank was closed to isolate the system from the ambient, and power input to the pressurization tank immersion heaters was regulated to maintain the desired system pressure.

Single-phase heat transfer data were obtained by operating at the lowest desired jet velocity and adjusting heater power to maintain a ΔT of approximately 10°C. When the system reached steady state the data were recorded and power was reduced by approximately 3 W. A second set of data was obtained in a similar fashion for the reduced power setting. The velocity was then increased slightly and the process repeated until velocities in a range from 0.5 to 12 m/s were covered. This procedure was repeated for a wide spectrum of nozzle inserts having slot widths of $W = 0.127$, 0.254, and 0.508 mm, and nozzle heights $H = 0.127$, 1.27, 2.54 and 5.08 mm. The inserts permitted variations in H/W in the range 1 to 20.

Determination of Temperature Distribution at the Heater Surface. Temperature measurements were obtained at a

Downloaded 17 Jul 2012 to 128.211.160.35. Redistribution subject to ASME license or copyright; see http://www.asme.org/terms/Terms_Use.cfm

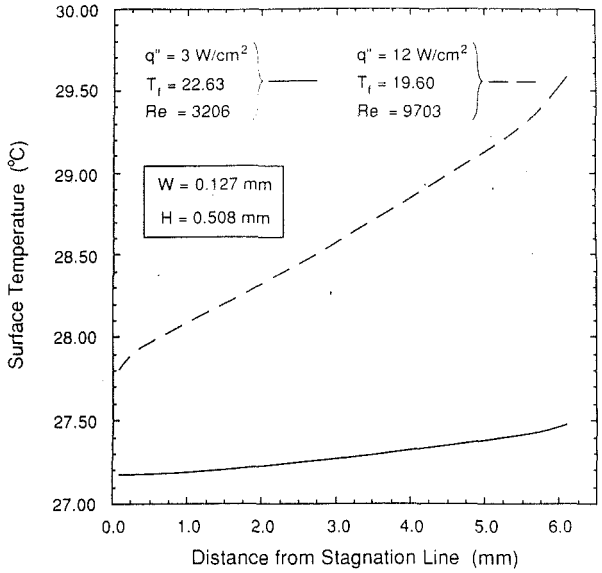

Fig. 5 Variation of chip surface temperature with distance from the impingement centerline

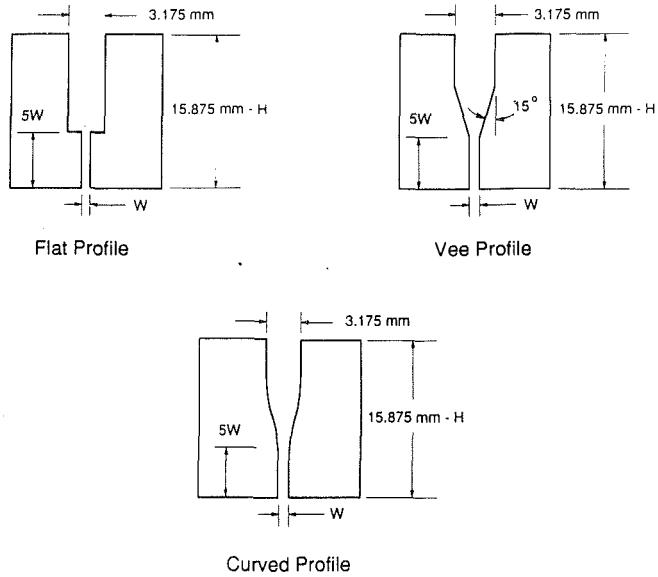

Fig. 6 Nozzle configurations

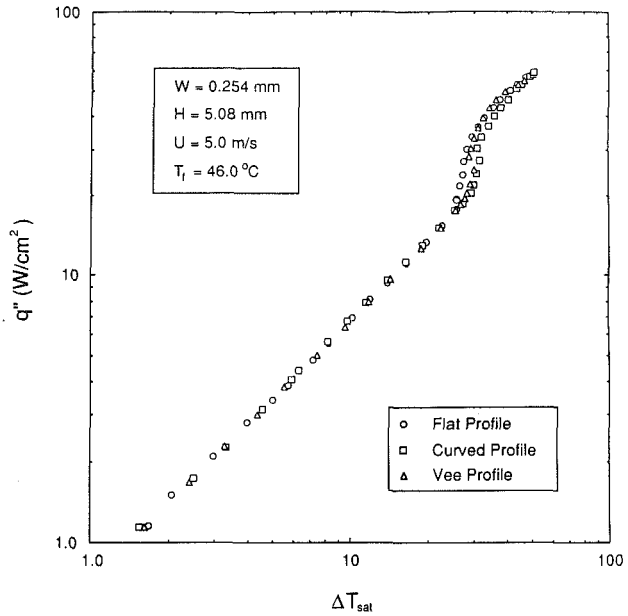

Fig. 7 Effect of nozzle shape on chip cooling performance

plane 0.812 mm below the heat transfer surface; therefore, it was necessary to correct the measured values to determine surface temperature distribution. Two different methods of correction were performed and compared for accuracy. The first method employed a simple one-dimensional correction and the second used a two-dimensional finite difference scheme described by Patankar (1980). For both cases the test heater was modeled to be symmetric about the impingement cenerline.

For the one-dimensional correction the heat flux at the thermocouple plane was assumed uniform, and the test heater was assumed perfectly insulated along its boundaries. Using Fourier's law of conduction, each of three measured temperatures at the thermocouple plane was corrected to its corresponding point on the surface. The average surface temperature was determined as an area-weighted average of the three corrected surface values.

The two-dimensional correction involved a two-step numerical procedure similar to that developed by Jiji and Dagan (1987). First, a temperature profile at the thermocouple plane was fitted to the three temperatures using a Gaussian interpolating polynomial. The temperature profile and heater power input were used in the finite-difference numerical program to predict the temperature field in the domain bound by the thermocouple plane and the back cover plate. Heat fluxes at each nodal point on the thermocouple plane were then computed based on the solved temperature field. One-dimensional conduction was next employed to obtain temperatures at the surface for each corresponding nodal point. The second step was to solve the entire test heater temperature domain (from the actual impingement surface to the back cover plate) using the corrected surface temperatures as a boundary condition in the two-dimensional model. Calculated temperatures at the thermocouple plane were then compared to the measured temperatures at the same locations. The differences between calculated and measured temperatures were within thermocouple measurement accuracy. The mean surface temperature predicted using the one-dimensional correction was within 4 percent of that predicted by the two-dimensional model. Based on these results it was determined that one-dimensional surface temperature correction was adequate.

Heat losses were estimated numerically by assigning zero values for contact resistances between the heater and the fiberglass insulation. This analysis gave an upper bound for the total heat loss since contact resistances reduce heat loss. The analysis showed that the heat loss was a maximum for the lowest heat transfer coefficient, approximately 4 percent, and asymptotically approached 1 percent for higher values of the heat transfer coefficient. Since the contact resistances could not be determined, the authors assumed in their calculations a total heat input equal to the electrical power supplied to the heater uncorrected for heat loss.

Individual measurement uncertainties of the voltage and current transducers, thermocouples, flow meter, geometric parameters, and the one-dimensional temperature correction between the thermocouple plane and the surface were determined and the propagation of these uncertainties to the values of $\overline{Nu}_L/Pr^{1/3}$ and Re were evaluated using the Taylor theorem and the Pythagorean summation of individual uncertainties. These techniques showed maximum uncertainties of 4.5 and 1 percent in determining the values of $\overline{Nu}_L/Pr^{1/3}$ and Re, respectively.

Figure 5 shows the variation of surface temperature with

Downloaded 17 Jul 2012 to 128.211.160.35. Redistribution subject to ASME license or copyright; see http://www.asme.org/terms/Terms_Use.cfm

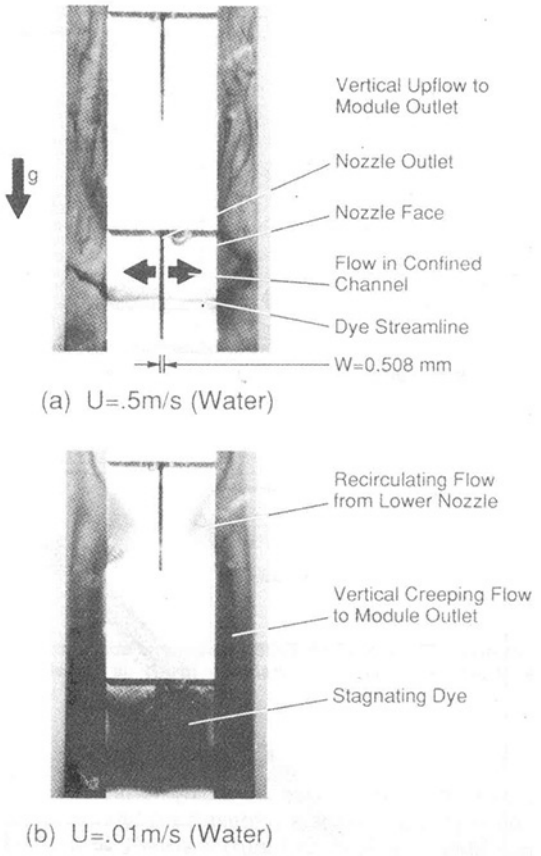

Fig. 8 Visualization of flow in the confinement channel for (*a*) $U = 0.50$ m/s and (*b*) $U = 0.01$ m/s

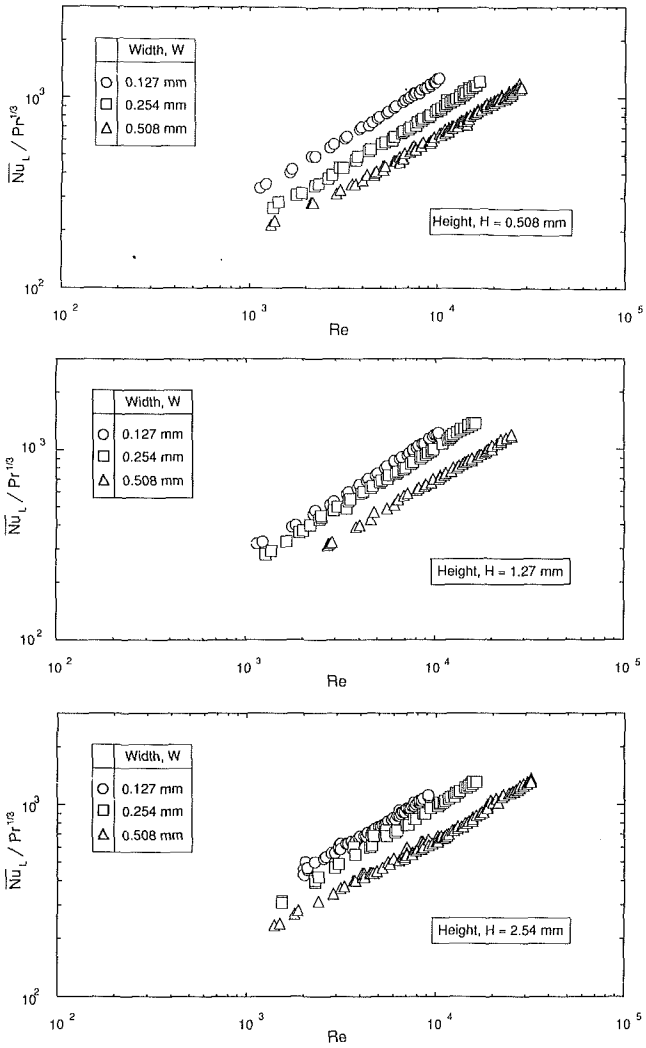

Fig. 9 Effect of Reynolds number and jet width on heat transfer for (*a*) $H = 0.508$ mm, (*b*) $H = 1.27$ mm, and (*c*) $H = 2.54$ mm

distance from the impingement centerline for different flow rates and inlet temperatures as predicted from the two-dimensional correction procedure. Each curve starts with a "cold" point corresponding to the impingement region, followed by a gradual increase in surface temperature with distance along the confinement channel. As expected the temperature gradient increases with increasing heat flux, but the surface temperature variation for the higher heat flux value is within a $\pm 1.8°C$ temperature band. This result represents strong evidence of the cooling uniformity associated with rectangular jets. This uniformity has, of course, been enhanced by the use of high-purity copper for heater construction. Since copper has approximately twice the thermal conductivity of the silicon used for making chips, multiplying the copper surface temperature variation band by a factor of two would suggest fairly isothermal surface conditions for silicon as well.

3 Results and Discussion

Effect of Nozzle Shape. Tests were conducted to evaluate the influence of the converging section of the nozzle on heat transfer performance. As shown in Fig. 6 three basic shapes were chosen for this comparative study. The width, W, and height, H, were held constant for each nozzle, and the straightening section was set at five times the nozzle width. Figure 7 shows full boiling curves obtained for nozzles with similar H and W, and identical values of jet velocity and inlet temperature. Each boiling curve was initiated in the single-phase region and concluded at the critical heat flux (CHF) point. Figure 7 displays no distinction between the heat transfer characteristics of the three nozzle shapes in the single-phase region. Small deviations occurred only in the boiling region (which is beyond the scope of the present study) until the three curves converged to unique values of critical heat flux and wall superheat. These results indicate that the short straightening section length to nozzle width ratio of five insured uniform flow conditions into the impingement zone and confinement channel. However, the flat and Vee profiles resulted in pressure drops that were, respectively, 15 and 5 percent higher than the curved profile. Thus it was decided that the Vee-profile would be used in the present study since it provided the best compromise between decreased pressure drop and ease of fabrication.

Flow Visualization. Flow uniformity in the cooling module was studied visually and with the aid of still and video photography. The electronic component and back cover plates were replaced with an optical-grade polycarbonate plastic cover, which permitted visual access to the impingement zone. A syringe needle inserted through the front cover plate injected dye into the convergent section of the nozzle. The dielectric fluid was replaced with water for these flow visualization experiments to avoid contamination of the expensive test fluid. The video system traced the path of the streamline of dye as it exited the nozzle, impinged on the polycarbonate window, and proceeded to the module outlet.

Figures 8(a) and 8(b) display traces of dye at jet velocities of 0.5 and 0.01 m/s, respectively. The dye streamline corresponding to the higher velocity follows a uniform horizontal path unaffected by gravity before exiting into the upflow channel. Close examination of the dye streamline by means of

Downloaded 17 Jul 2012 to 128.211.160.35. Redistribution subject to ASME license or copyright; see http://www.asme.org/terms/Terms_Use.cfm

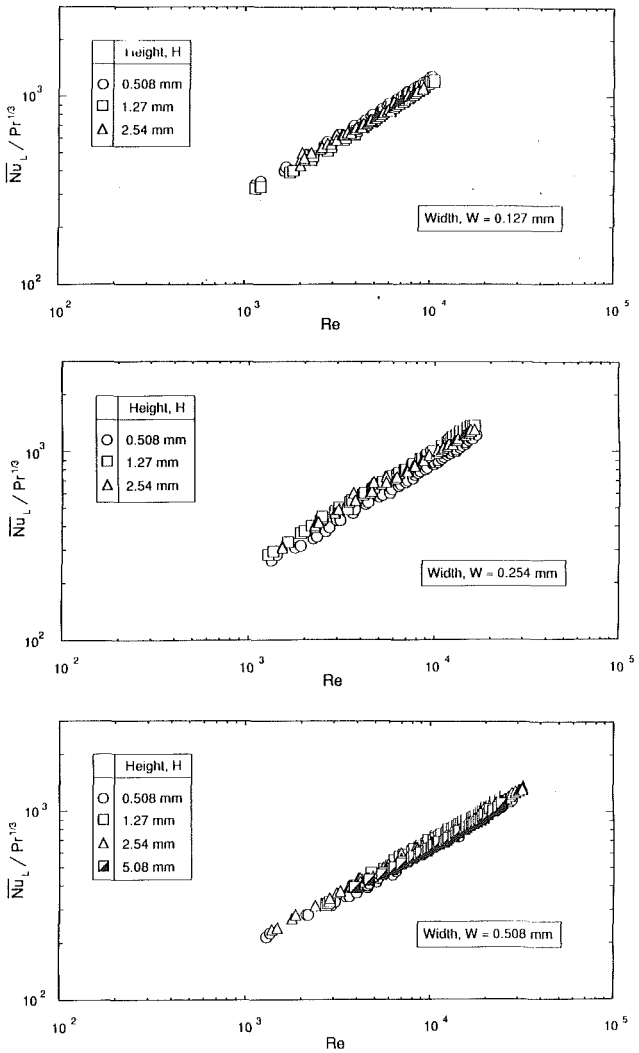

Fig. 10 Effect of Reynolds number and confinement channel height on heat transfer for (a) $W = 0.127$ mm, (b) $W = 0.254$ mm, and (c) $W = 0.508$ mm

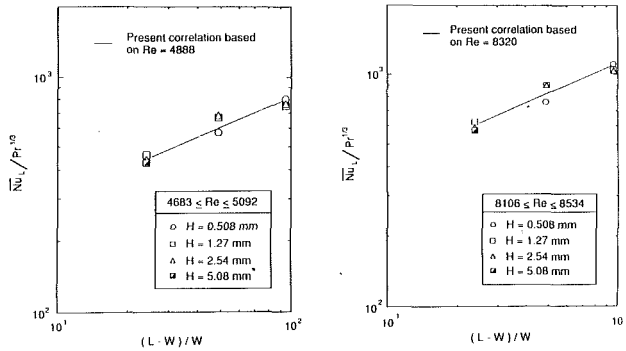

Fig. 11 Variation of the average Nusselt number with the ratio $(L - W)/W$

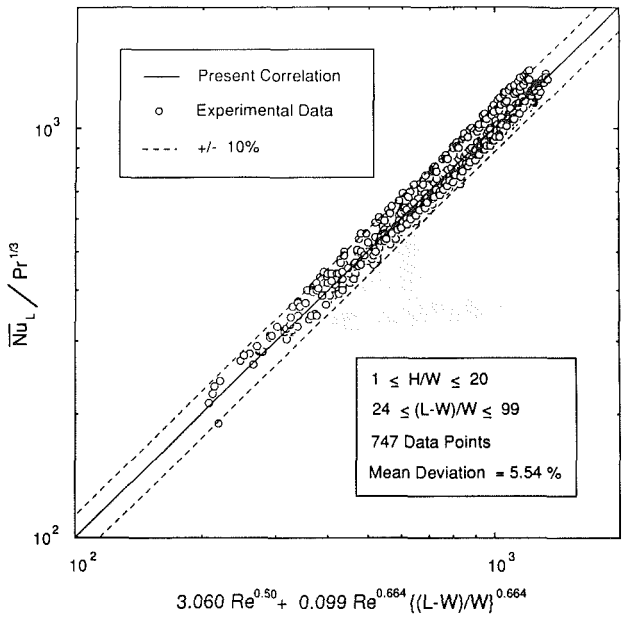

Fig. 12 Correlation of all the present single-phase heat transfer data

both still and video photography showed evidence of strong attachment of the streamline to the transparent cover surface. Figure 8(*b*) shows an extremely small jet velocity (0.01 m/s) inducing stagnation and recirculation in the confinement channel, as well as recirculation from the vertical upflow channel into the confinement channel of the jet vertically above the dyed jet. Transition to the streamlined conditions of the higher velocity case occurred at jet velocities slightly greater than 0.01 m/s.

The flow visualization experiments demonstrate a need for avoiding very small flow velocities to insure uniform and predictable cooling. Fortunately, the need to achieve heat fluxes commensurate with projected cooling loads for high power chips imposed a lower bound on jet velocity of approximately 1.0 m/s, two orders of magnitdue greater than the velocity corresponding to Fig. 8(*b*). This large velocity difference is a partial justification for drawing qualitative conclusions concerning FC-72 flow uniformity from flow visualization experiments performed with water. In any case, the 3×3 chip array was tested for cooling uniformity through heat transfer measurements obtained simultaneously for the nine chips. These multichip results will be discussed later in this section.

Heat Transfer Results. Figures 9 and 10 show data for ten different nozzle configurations. The data are grouped in two different ways, according to height and according to width. The plots reveal a relatively strong heat transfer dependence on nozzle width and virtually no dependence on channel height. This proves that for the conditions of the present study, the flow displays strong attachment to the impingement surface, and the other channel wall plays a minor role in influencing the flow. This statement is further substantiated in Fig. 11, which shows that heat transfer rate is independent of channel height.

The present data were reduced using a superposition technique commonly employed for correlating jet impingement data (Sitharmayya and Raju, 1969; Nakatogawa et al., 1970). This technique involves dividing the heated surface area into two regions: one, directly below the jet, dominated by jet impingement heat transfer, and a second region that extends beyond the impingement region.

The parameter $(L-W)/W$ in Fig. 11 was derived by dividing the heat transfer surface in the present study into two regions: one region, of width W, dominated by jet impingement, and a second region, of width L-W, governed by liquid flow at velocity U parallel to the chip surface. The entire data base of the present study was reduced using this superposition correlation technique. As shown in Fig. 12, the data were fitted by the equation

$$\overline{\mathrm{Nu}}_L/\mathrm{Pr}^{1/3} = 3.06\ \mathrm{Re}^{0.50} + 0.099\ \mathrm{Re}^{0.664}[(L-W)/W]^{0.664} \quad (1)$$

Downloaded 17 Jul 2012 to 128.211.160.35. Redistribution subject to ASME license or copyright; see http://www.asme.org/terms/Terms_Use.cfm

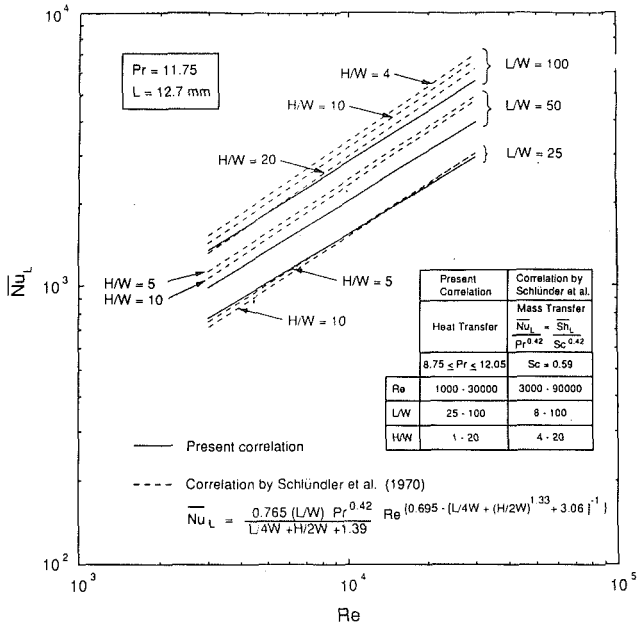

Fig. 13 Comparison of present correlation predictions with those of the Schlunder et al. (1970) correlation for mass transfer to a free gaseous jet

Table 1 Multichip heat transfer results ($W = 0.508$ mm, $H = 2.54$ mm)

Heater Arrangement

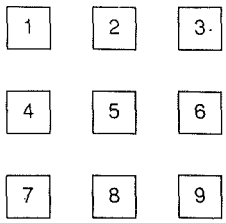

Heater Number	Re	$\overline{Nu}_L$	% Deviation*	Re	$\overline{Nu}_L$	% Deviation*	Re	$\overline{Nu}_L$	% Deviation*
1	9529	648.0	-1.36	11876	734.7	-1.79	14374	836.5	-0.13
2	9638	635.1	-3.97	11924	724.4	-3.40	14956	843.8	-1.59
3	9663	663.2	0.12	11915	758.9	1.24	14977	865.0	0.79
4	9699	648.5	-2.76	11937	732.2	-2.42	15079	841.5	-2.34
5	9680	631.2	-4.81	11891	722.3	-3.52	15037	838.1	-2.57
6	9782	623.5	-6.55	11892	719.0	-3.97	15103	815.8	-5.41
7	9702	651.3	-1.91	11798	725.7	-2.62	15069	818.0	-5.03
8	9688	649.8	-2.05	11669	721.1	-2.60	14982	842.0	-1.91
9	9713	645.9	-2.78	11594	698.6	-5.28	15077	820.6	-4.76

* % Deviation = $(\overline{Nu}_L - \overline{Nu}_{L,corr}) / \overline{Nu}_{L,corr} \times 100$; where $\overline{Nu}_{L,corr}$ is the average Nusselt number determined from the present correlation of heater no. 5 data

with a mean deviation (from the correlation) of 5.54 percent. Equation (1) is valid for Reynolds numbers ranging from 1000 to 30,000, and H/W values from 1 to 20. The Prandtl number exponent was fixed at 1/3 due to the limited variation in Prandtl number associated with the data. Dividing the heat transfer surface area into the aforementioned regions actually enhanced correlation accuracy. Attempts at modifying the exponent of the parameter $(L-W)/W$ from that of the Reynolds number in the second right-hand-side term of equation (1) actually increased the magnitude of deviation from the correlation.

It is important to note that, for small values of W, the second term on the right-hand side of equation (1) has a stronger effect on $\overline{Nu}_L$ than the jet impingement term. Hence, for very small values of W (i.e., $W \ll L$), equation (1) yields

$$\bar{h}_L \propto U^{0.664} L^{-0.336} \tag{2}$$

independent of jet width.

The EDM machining process utilized in fabricating the nozzle inserts of the present study imposes 0.03 mm as a minimum practical slot width. Using this width as a reference, and a heater length of 12.7 mm, which is typical of electronic chips, shows that the jet impingement term of equation (1) accounts for only 13.9 and 8.4 percent of the sum of the superposition terms for $Re = 1000$ and 30,000, respectively.

Equation (2) demonstrates that, for given fluid properties and chip length, the cooling rate can be increased by increasing jet velocity. The coolant flow rate may be minimized by reducing jet width without compromising chip cooling as long as jet velocity is set to the desired value. It is important to note that the pressure drop across the jet and confinement channel never exceeded 20 psi for the conditions of the present study. For a fixed flow rate of 0.043 gpm per chip, reducing nozzle width from 0.127 mm ($U = 0.413$ m/s) to 0.127 mm ($U = 1.69$ m/s) increased the pressure drop from less than 0.01 psi to only 0.10 psi. The highest pressure drop value of 20 psi was achieved at a flow rate of 0.38 gpm per chip using the smallest jet with of 0.127 mm (i.e., $U = 15$ m/s).

Figure 13 shows a comparison of predictions based upon the present correlation to those of the Schlunder et al. (1970) correlation for mass transfer to a free gaseous jet. The fair agreement between the two correlations is further evidence that, for conditions of the present study, the nozzle confinement plate has a weak effect on fluid flow and, therefore, the heat transfer is independent of channel height. As the ratio $(L-W)/W$ decreases, which corresponds to an increasing jet width, the heat transfer becomes more dominated by impingement, resulting in better agreement between the two correlations.

Module Cooling Uniformity. The heat transfer results of tests performed using the cooling module with a 3×3 array of simulated chips are detailed in Table 1. The heat transfer data for each of the nine chips are compared to values determined from equation (1) for the corresponding Reynolds number. Except for one measurement, the deviations of individual chip data from the correlation were less than the mean deviation associated with generating the correlation itself using heater number 5 data. These results strongly support the feasibility of using the present jet-impingement geometry and cooling module packaging technique to insure cooling uniform for large arrays of chips.

4 Summary

Experiments were performed to investigate single-phase heat transfer from a smooth 12.7×12.7 mm^2 simulated chip to a two-dimensional jet of dielectric Fluorient FC-72 liquid issuing from a thin rectangular slot into a channel confined between the chip surface and nozzle plate. Specific findings from the study are also as follows:

1 Cooling via rectangular jets maintains nearly isothermal chip surface conditions.

2 A nozzle straightening second 5 times the nozzle width provides uniform flow into the impingement region regardless of the nozzle inlet geometry. The choice of nozzle shape may therefore be based solely on the considerations of pressure drop and ease of fabrication.

3 The combined jet impingement/confinement channel configuration provides uniform and predictable flow parallel to the chip surface.

4 The chip cooling rate is independent of channel height for the conditions of the present study. The average Nusselt number is more strongly dependent upon jet velocity and jet width.

Downloaded 17 Jul 2012 to 128.211.160.35. Redistribution subject to ASME license or copyright; see http://www.asme.org/terms/Terms_Use.cfm

5 The chip cooling rate is determined by the contributions of a jet impingement region and region of flow parallel to the chip surface. A correlation based upon this superposition scheme was found successful at fitting all the data of the present study with a mean deviation of 5.54 percent. The correlation yields a vanishing effect of jet width on average chip heat transfer coefficient for small values of jet width. Thus, the chip cooling rate may be increased by increasing jet velocity alone. At the same time, the cooling flow rate may be minimized by reducing jet width without compromising chip cooling as long as jet velocity is set to the desired value.

6 The multijet cooling module is very successful in insuring equal flow distribution and heat dissipation from each of the nine simulated chips. The agreement between heat transfer data obtained for each of the nine chips with the correlation based on single chip data is strong evidence that the present module geometry is feasible for cooling large arrays of chips.

Acknowledgments

This material is based upon work supported by the National Science Foundation under Grant No. CBT-8618949. The authors appreciate this support and thank the Industrial Chemical Products Division of 3M for providing test fluid (FC-72) samples for the present study.

References

Bar-Cohen,, A., Mudawar, I., and Whalen, B., 1986, "Future Challenges for Electric Cooling," *Research Needs in Electronic Cooling*, F. P. Incropera, ed., published by the National Science Foundation and Purdue University, pp. 70–77.

Downs, S. J., and James, E. H., 1987, "Jet Impingement Heat Transfer—A Literature Survey," ASME Paper No. 87-HT-35.

Goldstein, R. J., and Timmers, J. F., 1982, "Visualization of Heat Transfer From Arrays of Impinging Jets," *Int. J. Heat Mass Transfer*, Vol. 25, pp. 1857–1868.

Jiji, L. M., and Dagan, Z., 1987, "Experimental Investigation of Single Phase Multi-Jet Impingement Cooling of Array of Microelectronic Heat Sources," *Proc. Int. Symp. on Cooling Technology for Electronic Equipment*, Honolulu, HI, pp. 265–283.

Ma, C. F., and Bergles, A. E., 1983, "Boiling Jet Impingement Cooling of Simulated Microelectronic Chips," *Heat Transfer in Electronic Equipment*, ASME HTD-Vol. 28, pp. 5–12.

Maddox, D. E., and Mudawar, I., 1989, "Single and Two-Phase Convective Heat Transfer From Smooth and Enhanced Microelectronic Heat Sources in a Rectangular Channel," ASME JOURNAL OF HEAT TRANSFER, Vol. 111, pp. 1045–1052.

Mudawar, I., and Anderson, T. M., 1989, "High Flux Electronic Cooling by Means of Pool Boiling—Part I: Parametric Investigation of the Effects of Coolant Variation, Pressurization, Subcooling and Surface Augmentation," *Heat Transfer in Electronics*, R. K. Shah, ed., ASME HTD-Vol. 111, pp. 35–50.

Mudawar, I., and Maddox, D. E., 1989a, "Critical Heat Flux in Subcooled Flow Boiling of Fluorocarbon Liquid on a Simulated Electronic Chip in a Vertical Rectangular Channel," *Int. J. Heat Mass Transfer*, Vol. 32, pp. 379–394.

Mudawar, I., and Maddox, D. E., 1989b, "Enhancement of Critical Heat Flux From High Power Microelectronic Heat Sources in a Flow Channel," *Heat Transfer in Electronics*, ASME HTD-Vol. 111, pp. 51–58.

Nakatogawa, T., Nishiwaki, N., Hirata, M., and Torri, K., 1970, "Heat Transfer of Round Turbulent Jet Impinging Normally on a Flat Plate," *Proc. 4th Int. Heat Transfer Conf.*, Paris-Versailles, France, Vol. 2, pp. 1–11.

Patankar, S. V., 1980, *Numerical Heat Transfer and Fluid Flow*, Hemisphere Publishing Corp., New York.

Ramadhyani, S., and Incropera, F. P., 1987, "Forced Convection Cooling of Discrete Heat Sources With and Without Surface Enhancement," *Proc. Int. Symp. on Cooling Technology for Electronic Equipment*, Honolulu, HI, pp. 249–264.

Samant, K. R., and Simon, T. W., 1986, "Heat Transfer From a Small, High-Heat-Flux Patch to a Subcooled Turbulent Flow," ASME Paper No. 86-HT-22.

Schlunder, E. U., Krotzch, P., and Hennecke, F. W., 1970, "Gesetzmassigkeiten der Warme- und Stoffubertragung bei der Prallstromung aus Rund- und Schlitzdusen," *Chemie Ingenieur Technik*, Vol. 42, pp. 333–338.

Sitharmayya, S., and Raju, K. S., 1969, "Heat Transfer Between an Axisymmetric Jet and a Plate Held Normal to the Flow," *The Canadian Journal of Chemical Engineering*, Vol. 47, pp. 365–368.

Downloaded 17 Jul 2012 to 128.211.160.35. Redistribution subject to ASME license or copyright; see http://www.asme.org/terms/Terms_Use.cfm